The Aeronautical Journal (2026), **130**, pp. 2293–2318
doi:10.1017/aer.2026.10157

RESEARCH ARTICLE

Cruise range modeling of a transport aircraft using machine learning

S. Mert Özer[1] and Tolga Baklacioglu[2]

[1]Aeronautical Engineering, Eskisehir Technical University, Eskisehir, Türkiye
[2]Aerospace Engineering, Eskisehir Technical University, Eskisehir, Türkiye
Corresponding author: Tolga Baklacioglu; Email: tbaklacioglu@eskisehir.edu.tr

Received: 1 May 2025; **Revised:** 27 February 2026; **Accepted:** 3 March 2026

Keywords: aircraft; cruise flight programmes; cruise range; energy efficiency; regression

Abstract

Accurate estimation of an aircraft cruise range is a critical challenge in aeronautical engineering that directly influences fuel efficiency, operational costs and environmental sustainability. Traditional analytical models, such as the Bréguet range equation, provide simplified range estimates but often fail to capture the nonlinear dependencies between flight parameters, fuel consumption and aerodynamic efficiency. In this study, machine learning-based regression methods have been employed to model the aircraft cruise range using the cruise flight data of Boeing 737–400, which is one of the most widely used commercial aircraft. Based on the calculated performance metrics, it is determined that the Gaussian process regression model exhibits superior validation and test performance compared to the other models. The developed models provide deeper insight into range variations under various flight conditions by performing accurate and robust predictions.

Nomenclature

R	Cruise range
V	True airspeed
c_T	Thrust-specific fuel consumption
L	Lift force
D	Drag force
L/D	Lift-to-drag ratio
W	Aircraft weight
W_0	Initial aircraft weight
W_1	Final aircraft weight
H	Range factor
S	Wing reference area
ρ	Air density
C_L	Lift coefficient
C_D	Drag coefficient
C_{D0}	Parasite drag coefficient
K	Induced drag coefficient
$\dot{m}_f$	Fuel mass flow rate
T	Engine thrust
h	Altitude
V_0	Initial airspeed
μ_k	Mean of kth predictor
σ_k	Standard deviation of kth predictor
$\bar{x}_k$	Normalized predictor

© The Author(s), 2026. Published by Cambridge University Press on behalf of Royal Aeronautical Society.

https://doi.org/10.1017/aer.2026.10157 Published online by Cambridge University Press

x_k	Predictor variable
n	Number of samples
p	Number of predictors
y_i	Actual value
$\hat{y}_i$	Predicted value
$\bar{y}$	Mean of actual values
R^2	Coefficient of determination
MSE	Mean squared error
RMSE	Root mean squared error
MAE	Mean absolute error
N	Number of observations

1.0 Introduction

The prediction of aircraft range is a fundamental problem in aeronautical engineering that affects fuel efficiency, operational costs and environmental impact. Furthermore, the ability to estimate the cruise range is essential for aircraft design, performance assessment, flight planning and trajectory prediction. Traditionally, range prediction has relied on analytical models such as the Bréguet range equation and range integration methods, which provide simplified approximations for fuel consumption and range performance [1]. Although these classical models have been extensively used, they fail to capture the full complexity of real-world flight conditions, including aerodynamic nonlinearities, changing fuel consumption rates and operational constraints. Therefore, more advanced methods must be developed to achieve more efficient flight operations, as they directly inform decisions that optimise fuel consumption and reduce emissions.

Fuel consumption can be thought of as a key determinant of the operational range of an aircraft, which directly influences cost efficiency, emissions and overall performance. The fuel flow rate varies significantly between different flight phases and affects the total fuel required for a given mission [2]. In Ref. [3], a detailed analysis of fuel flow during the cruise flight has been conducted that emphasises the importance of optimising altitude and speed to minimise fuel burn. In Refs [4–6] machine learning-based neural network models are developed to accurately predict fuel consumption patterns to improve fuel efficiency estimates for commercial aircraft. In particular, the cost index optimisation can lead to a significant reduction in fuel use [7]. In this regard, the development of an accurate cruise range model would be also beneficial for the convergence capability of fuel consumption prediction models.

On the other hand, aircraft emissions is an important environmental concern, with carbon dioxide (CO_2), nitrogen oxides (NO_x) and particulate matter being the main contributors to climate change and local air pollution [8]. Since the fuel consumption of an aircraft is directly related to its range, optimising cruise flight programmes can reduce emissions while extending the maximum cruise range. Therefore, the choice of cruise flight programme plays a crucial role in both fuel efficiency and emissions. Studies have shown that cruise altitude, airspeed and weight all influence the amount of CO_2 released during flight [9]. In addition, aircraft with improved aerodynamic efficiency and optimised weight distribution emit less CO_2 per unit of range [10]. Even unmanned aerial vehicles exhibit variations in emissions based on their flight profile and weight, reinforcing the need for precise fuel consumption modeling [11]. Consequently, a machine learning-based cruise range estimation model is crucial as it can lead to both fuel-efficient and lower-emission flight strategies by predicting optimal flight parameters more accurately than traditional models.

1.1 Literature review on aircraft range estimation

Aircraft range estimation has been widely studied using both classical analytical models and modern computational approaches. Bréguet's range equation, originally developed in the early 20th century,

https://doi.org/10.1017/aer.2026.10157 Published online by Cambridge University Press

remains a widely used theoretical framework for estimating range based on lift-to-drag ratio, fuel weight and specific fuel consumption [12]. Over the years, several refinements have been made to improve its predictive accuracy. In Ref. [13], the Bréguet range equation is extended by incorporating compressibility effects and cambered wing drag polars, making it more applicable to high-subsonic-transport aircraft. In Refs [14, 15], on the other hand, approximate range solutions are further developed for constant altitude and constant speed cruise flights, which are more representative of modern aircraft operations.

There are also studies that focus on improving range estimates by considering real-world operational constraints. In Ref. [16], the concept of a specific range, which provides an instantaneous measure of distance per unit of fuel consumed, is proposed to offer an alternative to the integrated range equations described in Ref. [1]. Cruise performance and range prediction are revisited by incorporating compressibility effects and proposing a non-iterative fuel estimation procedure [17]. In Ref. [18], it is demonstrated that maximum range is highly sensitive to atmospheric conditions, especially the effect of wind. In Ref. [19], flight data recorder (FDR) measurements are used to refine fuel burn estimates. It is shown that traditional range equations underestimate fuel consumption in real-world operations. In Ref. [20], quick access recorder (QAR) data is utilised to improve the drag polar and thrust-specific fuel consumption models, and subsequently applied the Bréguet range equation for enhanced cruise range prediction. In Ref. [21], on the other hand, the maximum range and airspeed of a commercial aircraft are estimated considering the presence of transonic wave drag, thereby improving prediction accuracy.

It is well known that the weight of an aircraft is a critical determinant of its range, which influences fuel consumption, aerodynamic efficiency and operational flexibility. The takeoff weight, which includes payload, fuel and operating empty weight, directly affects the range calculations. In this regard, many studies have shown that accurate weight estimation is essential for trajectory modeling and fuel burn prediction [22]. Traditional range models such as the Bréguet range equation, however, assume a continuous weight reduction due to fuel consumption, yet recent approaches have improved aircraft mass estimation during different flight phases, leading to more precise range predictions [23]. Furthermore, fuel weight estimation models, particularly for military aircraft, demonstrate that the fuel-to-weight ratio significantly impacts endurance and operational efficiency [24]. These findings emphasise the need for advanced predictive models that can dynamically estimate aircraft weight and its effect on range. In practice, the specific fuel consumption varies with thrust, airspeed and altitude, and this behaviour plays an important role in determining accurate range predictions. Several studies, such as Refs [18, 25], discuss these functional dependencies, which are typically simplified or neglected in classical Bréguet-type analyses.

Optimisation-based techniques (especially metaheuristic methods such as genetic algorithms (GA) and particle swarm optimisation (PSO)) have also been employed to improve range estimates. GA and PSO are used to develop non-linear models that estimate the cruise range based on velocity, weight and altitude (see Subsection 2.2 for details) [26]. Although these methods offer improved accuracy compared to analytical models, they are computationally expensive and sensitive to hyperparameter selection. In addition, those models are developed for specific altitudes that do not allow us to predict range values of different altitudes. On the other hand, the potential of machine learning for range prediction is demonstrated in Refs [27, 28] by proposing data-driven optimisation frameworks that integrate real-world flight data into mission analysis algorithms.

Recent advances in machine learning have introduced new possibilities for modeling aircraft performance. For example, in Ref. [29], an iterative convex programming approach is developed for the prediction of the range of electric aircraft that outperforms classical models by incorporating battery discharge dynamics. Similarly, in Ref. [30], a hybrid electric Bréguet range equation is formulated to predict the range of hybrid electric aircraft. In Ref. [28], a data-driven flight simulation framework is proposed to enhance range predictions by using supervised learning techniques. In Ref. [19], a data-enhanced Bréguet range model is introduced using a hybrid approach that combines physics-based models with machine learning corrections.

https://doi.org/10.1017/aer.2026.10157 Published online by Cambridge University Press

1.2 Objectives

In light of the literature review, the present study aims to improve aircraft range modeling by using machine learning-based regression models (which have never been used to the best knowledge of the authors) to achieve more accurate and data-driven range predictions. Therefore, it is aimed to use the cruise flight data of Boeing 737–400 given by its Operations Manual [31]. In case of absence of FDR or QAR data of an aircraft, developing a highly convergent regression model based solely on the Operations Manual data is extremely vital since the developed methodology would still be valid and accurate. The key objectives can be listed as:

- To model, train and validate multiple machine learning-based regression models for range estimation under two different cruise flight programmes, namely *the constant speed and constant lift coefficient* and the constant altitude and constant lift coefficient.
- To determine the best regression model for range estimation regarding certain performance metrics calculated for the validation and test data.
- To gain insight into the performance of the present aircraft by performing range predictions for various altitudes with changing velocity and weight parameters.

The last item of the above list is particularly valuable as there is limited information in the Operations Manual of the aircraft.

It should be noted that the study focuses on predicting steady-state cruise range rather than modeling the full evolution of the flight. Unlike analytical range formulations, the proposed machine learning approach does not describe the continuous variation of state variables but instead captures the steady-flight relationships that govern cruise performance.

In addition, in this study, range is modelled rather than optimised; that is, the cruise performance is predicted under prescribed flight conditions without seeking flight profiles that maximise range. Optimisation-based approaches rely on direct or indirect optimal control methods (e.g., Refs [32, 33], which are outside the scope of this work.

1.3 Paper structure

The rest of this paper is structured as follows: Section 2 presents the existing cruise range formulations for two different cruise flight programmes. In Section 3, the main contribution of the study is presented. First, the main parts of the regression modeling workflow are introduced. Then, the results of the training and validation phases are presented over the calculated performance metrics and visualisation. In Section 4, the machine learning range predictions are compared with analytical range formulations to provide physical insight and illustrate where the classical equations diverge from real performance due to their simplifying assumptions. In Section 5, the trained machine learning models are used to predict cruise range for unseen operating conditions to evaluate their generalisation capability beyond the training data. In Section 6, the concluding remarks are given along with future research directions.

2.0 Cruise range formulations for different cruise flight programmes

Range is a basic operational requirement and design criterion, especially for transport category aircraft. Due to this importance, range performance has been extensively studied by numerous researchers since the early days of aviation [12, 14, 19]. This section presents the fundamental range equations for different cruise flight programmes employed by jet-powered aircraft.

The analytical formulations presented in the following subsection are included to introduce the two distinct cruise flight programmes commonly employed in range analysis and to clarify how key parameters influence the cruise range. Specifically, these formulations serve to highlight the role of velocity, altitude, lift-to-drag ratio and fuel consumption in shaping range performance, thereby offering a physical perspective on the problem addressed in this study.

https://doi.org/10.1017/aer.2026.10157 Published online by Cambridge University Press

2.1 Analytical range formulations

The constant velocity and constant lift coefficient cruise, commonly known as climbing-cruise flight, represents the optimal trajectory for long-range, high-subsonic-speed flight. The Bréguet range equation applies to this cruise flight programme:

$$R = \frac{V}{c_T}\frac{L}{D}\ln\frac{W_0}{W_1} \tag{1}$$

where R is the range, V is the true airspeed, c_T is the specific fuel consumption, L and D are the lift and drag forces acting on the aircraft, respectively, W_0 is the initial weight of the aircraft and W_1 is the final weight of the aircraft [12, 14].

For constant airspeed, lift-to-drag ratio, and specific fuel consumption during cruise, the equation can be expressed in terms of the range factor H:

$$R = H\ln\frac{W_0}{W_1}. \tag{2}$$

where H represents the nominal aircraft performance during cruise and is equal to:

$$H = \frac{V\,(L/D)}{c_T}$$

This climbing-cruise flight strategy allows aircraft to maintain optimal lift-to-drag ratio as fuel burns off by gradually increasing altitude, theoretically maximising range. However, it is rarely fully implemented in practice due to existing air traffic control constraints [15].

The constant altitude and constant lift coefficient cruise range of a jet-powered aircraft is given by:

$$R = \frac{2\,(L/D)}{c_T}\sqrt{\frac{2}{\rho S C_L}}\left(\sqrt{W_0} - \sqrt{W_1}\right) \tag{3}$$

or alternatively expressed in a more practical form:

$$R = \frac{2\,(L/D)}{c_T}V_0\left(1 - \sqrt{\frac{W_1}{W_0}}\right) \tag{4}$$

where

$$V_0 = \sqrt{\frac{2W_0}{\rho S C_L}}$$

is the initial airspeed calculated at the beginning of the cruise [13, 19]. In these equations, S represents the wing reference area, ρ is the air density and C_L is the lift coefficient.

This cruise involves maintaining a constant altitude while the aircraft weight decreases due to fuel burn, resulting in a gradually decreasing airspeed to maintain the constant lift coefficient [15, 19]. It should be noted that this approach is less favoured in practice due to operational constraints, including fixed schedules and speed requirements.

While the range formulations expressed in (1) and (3) are useful for illustrating how cruise range depends on velocity, altitude, lift-to-drag ratio and thrust-specific fuel consumption (TSFC), several drawbacks limit their applicability. First, the practical use of these equations requires a TSFC model that accounts for variations with altitude, Mach number and engine operating conditions. Deriving such a model with sufficient accuracy for the Boeing 737–400 is highly challenging in the absence of manufacturer data, and generic approximations would introduce inconsistencies. Second, an accurate drag polar model is needed to determine the aerodynamic efficiency L/D over the relevant cruise. However, the transonic flight regime of the 737–400 is strongly affected by compressibility effects, wave drag and aerofoil camber, which cannot be captured adequately by conventional quadratic drag polar approximations of the form

$$C_D = C_{D0} + KC_L^2 \tag{5}$$

https://doi.org/10.1017/aer.2026.10157 Published online by Cambridge University Press

where C_D represents the drag coefficient, C_{D0} is the parasite drag coefficient and K indicates the induced drag coefficient. These second-order polars are well suited for incompressible or low-speed flows but are known to underestimate drag rise in the transonic regime, thereby leading to optimistic and physically unrealistic range predictions.

Consequently, applying Equations (1) and (3) with such simplified aerodynamic and propulsion models would yield misleading results. To overcome these limitations, the present study adopts a data-driven regression methodology, which directly learns the input–output mapping from the Boeing 737–400 Operations Manual dataset (see Section 3). By doing so, the combined effects of TSFC variation, aerodynamic nonlinearities and operational constraints are inherently embedded in the model, eliminating the need for explicit but often inaccurate analytical approximations. In this respect, Section 4 presents a comparison between the analytical and real range values, illustrating how the analytical formulas begin to deviate from the Operational Manual data due to their underlying simplifications.

2.2 Non-conventional formulations

More recently, an innovative approach has been proposed, which models the range equations introduced in Subsections 2.1 using optimisation-based methods [26]. The proposed method presents two empirical formulas which are

$$R = a_1 V\sqrt{W} + b_1 \ln\left(V\sqrt{W}\right) + c_1 V\sqrt{W}\ln\left(V\sqrt{W}\right) + d_1 \tag{6}$$

for the constant altitude and constant lift coefficient cruise, and

$$R = a_2 W \arctan(W) + b_2 \arctan(W) + c_2 W + d_2 \tag{7}$$

for constant velocity and constant altitude cruise. These equations require coefficient optimisation for specific aircraft types and flight programmes. Unlike traditional analytical approaches, these models eliminate the need for detailed drag polar specifications while still accounting for the effects of modern transport aircraft's cambered wings and compressibility.

In Ref. [26], the coefficients of the formulas are found according to the operational data of a jet-powered aircraft using metaheuristic optimisation methods, such as GA and PSO. The error analysis revealed correlation coefficients very close to 1 for both cases. This performance validates these non-conventional approaches as powerful alternatives to traditional analytical range equations [26].

However, these models present several notable limitations. The most crucial limitation is that they are altitude-specific. To be more precise, each empirical formula is derived separately for a given altitude, requiring distinct optimisation of coefficients for each case. As a result, these models lack the ability to generalise across a continuous range of flight altitudes. Therefore, it is not possible to make range predictions for different altitudes, which significantly restricts their practical applicability in real-time flight planning and performance assessment.

In light of the above discussion, our aim is to obtain a unified regression model that captures the full variability of altitude, weight and speed within a single framework. In the next section, the proposed method is explained in detail.

3.0 Regression modeling of the cruise range

Given cruise flight data, the main objective is to model the range dynamics of the aircraft for two different cruise flight programmes. In order to obtain these models, we utilise machine learning-based regression modeling where the associated workflow of this process is illustrated in Fig. 1.

We apply the regression modeling workflow whose vital phases are explained in the following subsections. In a nutshell, the process begins with portioning the dataset into training/validation and testing subsets to facilitate model development and generalisation assessment. Then a normalisation is performed, where the predictor inputs are normalised to ensure uniform scaling. Within the validation subset, k-fold cross-validation is applied to evaluate the performance of different regression models.

https://doi.org/10.1017/aer.2026.10157 Published online by Cambridge University Press

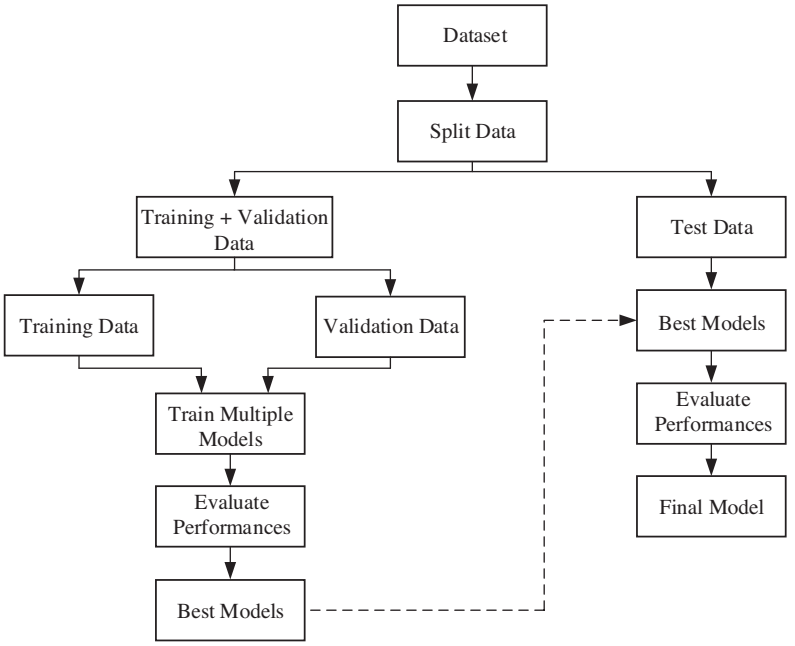


Figure 1. *Regression modeling workflow.*

The goal is to choose a few regression models that yield the best validation performance. Then, the performance of the chosen models is evaluated using the test data, which remain completely unseen during training and validation. According to the performance results, the best regression model is chosen. Once the regression is obtained, range values can be predicted for the given input data. It should be noted that the normalisation of validation, test and prediction data is performed according to the normalisation factors of the training data.

3.1 Dataset and assumptions

As in Refs [15, 26], we consider one of the most widely used jet-powered commercial aircraft – Boeing 737–400, whose technical specifications are given in Table 1. To model the range dynamics of the aircraft, we utilise the cruise flight data given by the Operations Manual [31]. The manual lists discrete combinations of range, aircraft weight, altitude and true airspeed. The Operations Manual provides the cruise performance data as direct tabulated values without any accompanying statistical information. These tables are given for the two cruise flight programmes, resulting in two distinct datasets used in this study. The relevant flight data give operational range values for two cruise flight programmes:

- Constant velocity and constant lift coefficient: a steady Mach number of $M = 0.74$ for altitudes from 21,000 ft to 37,000 ft.
- Constant altitude and constant lift coefficient: the variable Mach numbers for altitudes from 10,000 ft to 30,000 ft.

For the constant velocity and constant lift coefficient cruise, it should be noted that the aircraft does not operate at a fixed altitude in real flight. This cruise flight programme corresponds to a climb–cruise, in which the aircraft gradually increases its altitude as fuel is burned while maintaining constant velocity and lift coefficient. The altitude values provided in the Operations Manual therefore do not represent level cruise at a fixed altitude, nor a mean altitude over the entire cruise, but rather discrete reference altitude levels associated with representative climb–cruise conditions. These manufacturer-defined altitude

https://doi.org/10.1017/aer.2026.10157 Published online by Cambridge University Press

Table 1. *Specifications of the case study jet-powered commercial aircraft Boeing 737–400*

Aircraft characteristics	
Wing area	91.04 m^2
Wing sweepback at quarter-chord	25 deg
Average wing thickness/chord ratio	12.89%
Maximum take-off weight	68,038 kg
Maximum zero-fuel weight	53,070 kg
Engines	2 x CFM56-3-B1

Table 2. *Statistical properties of weight and range data for the constant velocity and constant lift coefficient cruise*

		Altitude			
		21,000ft	25,000ft	30,000ft	37,000ft
Weight (kg)	N	330	330	330	219
	Mean	51,450	51,450	51,450	46,000
	SD	9,541	9,541	9,541	6,336
	Min	35,000	35,000	35,000	35,100
	Max	67,900	67,900	67,900	56,900
Range (mile)	N	330	330	330	219
	Mean	2,387	2,710	3,102	2,466
	SD	1,359	1,527	1,715	1,343
	Min	0	0	0	0
	Max	4,676	5,251	5,897	4,631

levels are commonly used for practical performance assessment and serve as nominal reference points for range evaluation.

In Tables 2 and 3, the statistical properties of the cruise flight data are given according to two different cruise flight programmes introduced in Subsections 2.1. and 2.2, respectively. It should be noted that the difference in data density, i.e. N, is due to the Operations Manual itself; as shown in Tables 2 and 3, the manual provides less data for the constant altitude and constant lift coefficient cruise compared to the constant velocity and constant lift coefficient cruise.

Note that the values are generated by the manufacturer assuming the following:

- International Standard Atmosphere (ISA) conditions
- Zero wind and no temperature deviation
- Clean configuration (flaps retracted, gear up)
- No step-climb or air traffic control constraints
- Long-range cruise settings for the constant velocity and constant lift coefficient cruise, and maximum-range cruise settings for the constant altitude and constant lift coefficient cruise

Thus, the dataset represents idealised performance in still-air conditions, without operational factors such as cost-index optimisation or weather effects. By using these manufacturer-provided datasets, the present study ensures that the input–output pairs used for machine learning are internally consistent with a well-defined aerodynamic and propulsion baseline, while avoiding the need to explicitly determine lift, drag, and thrust-specific fuel consumption from separate sources.

https://doi.org/10.1017/aer.2026.10157 Published online by Cambridge University Press

Table 3. *Statistical properties of weight, true-air-speed (TAS) and range data for the constant altitude and constant lift coefficient cruise*

		Altitude			
		10,000ft	20,000ft	25,000ft	30,000ft
Weight (kg)	N	32	33	32	19
	Mean	50,500	51,000	50,500	46,053
	SD	9,380	9,669	9,380	5,720
	Min	35,000	35,000	35,000	37,000
	Max	66,000	67,000	66,000	56,000
TAS (knots)	N	32	33	32	19
	Mean	344.4	390.6	411.6	421.3
	SD	26.6	29.1	26.4	14.4
	Min	298	338	361	394
	Max	386	434	447	439
Range (mile)	N	32	33	32	19
	Mean	2,017	2,555	2,733	2,225
	SD	1,172	1,472	1,574	1,096
	Min	0	0	0	0
	Max	3,880	4,880	5,212	4,063

3.2 Splitting the dataset

To evaluate the generalisation performance of the regression models on unseen data, the complete dataset must be initially partitioned into two non-overlapping subsets. In this manner, 70/30 split is employed as a common practice, where 70% of the data is allocated for model development (training and validation), and the remaining 30% is reserved exclusively for testing.[1]

To ensure a reliable and unbiased model evaluation during training, the validation phase employs *k-fold cross-validation*, a well-established resampling technique to estimate the generalisation performance of supervised learning algorithms. In this method, the training dataset is randomly partitioned into k approximately equal-sized and mutually exclusive subsets, or 'folds'.

For each of the k iterations, one fold is reserved as the *validation set*, while the remaining $k-1$ folds are combined to form the *training set*. The model is trained on the training set and evaluated on the validation set. This process is repeated k times, so that each fold is used exactly once for validation.

The performance metric, e.g. R^2, MSE, RMSE (see Subsection 3.4), is computed in each iteration, and the overall validation score is obtained by averaging the results:

$$\text{Validation Score} = \frac{1}{k}\sum_{i=1}^{k}\mathcal{M}_i \tag{8}$$

where $\mathcal{M}_i$ denotes the performance metric computed on the i^{th} validation fold.

In this study, 10-fold cross-validation is employed. This procedure reduces variance and mitigates the risk of overfitting or underfitting associated with a single, arbitrary train–validation split. It provides a more robust estimate of predictive capability of the model on unseen data and is particularly advantageous when the available dataset is limited in size.

Once the optimal model configuration is selected based on cross-validation performance, it is retrained using the entire 70% training and validation subset and then evaluated on the 30% hold-out test set. This final evaluation provides an unbiased estimate of the predictive accuracy of the model on truly unseen data, simulating real-world deployment conditions.

[1] Note that it is also acceptable to use 80/20 split depending on the size of the dataset.

https://doi.org/10.1017/aer.2026.10157 Published online by Cambridge University Press

This two-phase evaluation, i.e. cross-validation for model selection and hold-out testing for generalisation assessment, offers a balanced trade-off between reliable validation and conservative performance reporting.

3.3 Normalisation

A normalisation procedure is utilised on the predictor inputs to ensure consistent scaling and improve model performance. In this sense, z-score normalisation (standardisation) is utilised. This preprocessing step is particularly important for models sensitive to feature magnitudes, i.e. the regression models introduced in Subsection 3.3.

For $k = 1, 2, \ldots, p$, where p is the number of predictors, let

$$\mathbf{x}^k = \left[x_1^k, x_2^k, \ldots, x_n^k\right]^T$$

denote the vector of the k^{th} predictor with n number of observations. z-score normalisation transforms each predictor vector, i.e. $\mathbf{x}^k$, to a normalised vector, to be defined as $\bar{\mathbf{x}}^k$, which has zero mean and unit variance. In this regard, for $i = 1, 2, \ldots, n$:

$$\bar{x}_i^k = \frac{x_i^k - \mu_k}{\sigma_k}$$

where μ_k and σ_k are the mean and standard deviation of $\mathbf{x}^k$. This ensures that all predictors contribute proportionally to model training, regardless of their original units or scales.

In this respect, the z-score normalisation is applied to the weight and speed data of two different cruise flight programmes. Consequently, each observation is normalised using the mean and SD values of the training data.

The response variable is kept in its original units, since normalisation is applied only to the predictor inputs. However, to ensure the validity and generalisability of the regression models, it is essential that the same normalisation procedure, i.e. z-score normalisation, is applied to each predictor input consistently across all phases: training, cross-validation, testing and prediction. Therefore, during the prediction phase (explained in Subsection 3.6), when unseen predictor inputs are provided, the same z-score normalisation will be applied to each predictor value using μ_k and σ_k for the k^{th} predictor of the training data. In this way, it is ensured that consistency between all phases of the process is established.

3.4 Model training and testing

In order to find the most accurate and robust predictive model for aircraft cruise range, multiple machine learning regression methods are trained and compared. This comparative approach is essential due to the varying characteristics of the available data and the different strengths and limitations of individual regression methods. Each model responds differently to nonlinearity, noise, dimensionality and data volume; therefore, evaluating several candidates provides a more reliable path toward optimal generalisation performance. In this phase, four different regression methods have been considered due to their diverse modeling capabilities and their proven effectiveness in previous studies related to engineering system modeling.

1. *Decision tree regression (DTR)* recursively splits data into homogeneous subgroups based on feature values, forming a tree-like structure. The model makes predictions by averaging the target values in each terminal node. By this way, it allows to handle nonlinear relationships naturally. Decision trees are interpretable and require minimal preprocessing. However, DTR is prone to overfitting, which causes instability to small variations in data.
2. *Support vector regression (SVR)* extends support vector machines to regression tasks by fitting a function within a specified ε-margin of tolerance. It minimises the error while maximising the margin between predictions and actual values. The use of kernel functions enables SVR

https://doi.org/10.1017/aer.2026.10157 Published online by Cambridge University Press

to model nonlinear relationships, making it robust to high-dimensional data. However, SVR is computationally expensive and requires careful tuning of hyperparameters.

3. *Gaussian process regression (GPR)* is a probabilistic regression method that models a distribution over functions rather than a single function. It provides both predictions and uncertainty estimates. Because of that, it is useful for Bayesian inference. GPR is highly flexible and can capture complex patterns through kernel functions. It is computationally expensive which makes it unsuitable for large datasets.
4. *Neural network regression (NNR)* is a deep learning-based approach that can approximate complex, nonlinear functions by learning hierarchical representations of data. It automatically captures intricate patterns without requiring manual feature engineering. Though NNR is highly powerful and scalable, neural networks are computationally intensive, require large amounts of data, and are often regarded as a black-box model due to their lack of interpretability.
5. Training and testing of these models are carried out using MATLAB, which provides a streamlined environment for supervised learning tasks, allowing efficient preprocessing, cross-validation, hyperparameter tuning and performance visualisation [34].

3.5 Model performance evaluation

Evaluating the performance of a regression model is crucial to understanding its accuracy, reliability and generalisation capability. Various metrics are used to quantify how well the predictions of a model align with the actual values. These metrics provide insights into model bias, variance and overall predictive performance. The most commonly used evaluation metrics for regression models are discussed below.

The coefficient of determination, denoted as R^2, measures the proportion of variance in the dependent variable explained by the model. For n samples,

$$R^2 = 1 - \frac{\sum_{i=1}^{n} (y_i - \hat{y}_i)^2}{\sum_{i=1}^{n} (y_i - \bar{y})^2} \tag{9}$$

where y_i and $\hat{y}_i$ are the actual and predicted target values, respectively. Furthermore, $\bar{y}$ is the mean of the actual target values. The value of R^2 can be interpreted as follows.

- $R^2 = 1$: The model explains all the variance (perfect fit).
- $R^2 = 0$: The model explains none of the variance.
- $R^2 < 0$: The model performs worse than predicting the mean.

The mean squared error (MSE) quantifies the average squared difference between the actual and predicted values. MSE can be calculated as

$$MSE = \frac{1}{n} \sum_{i=1}^{n} (y_i - \hat{y}_i)^2 \tag{10}$$

Therefore, a lower MSE indicates a better fit. Due to the squared error term, MSE is sensitive to outliers.

The root mean squared error (RMSE) is the square root of MSE, and defined as

$$RMSE = \sqrt{MSE} = \sqrt{\frac{1}{n} \sum_{i=1}^{n} (y_i - \hat{y}_i)^2} \tag{11}$$

RMSE represents the typical size of prediction errors which makes it more sensitive to outliers than MAE.

https://doi.org/10.1017/aer.2026.10157 Published online by Cambridge University Press

Table 4. *Cross-validation and test performance results for the constant velocity and constant lift coefficient cruise*

		Regression model			
		DTR	SVR	GPR	NNR
Validation	R^2	0.99	0.99	≈ 1	≈ 1
	MSE	4,909.5	15473	0.75	107.66
	RMSE	70.06	124.39	0.87	10.37
	MAE	57.76	110.63	0.5	4.01
Test	R^2	0.99	0.99	≈ 1	≈ 1
	MSE	4,409.7	14070	0.72	5.69
	RMSE	66.4	118.62	0.85	2.38
	MAE	54.22	102.56	0.48	1.84

The mean absolute error (MAE) measures the average absolute difference between actual and predicted values, and defined as

$$MAE = \frac{1}{n}\sum_{i=1}^{n}\left|y_i - \hat{y}_i\right| \tag{12}$$

Since MAE gives equal weight to all errors, it is less sensitive to large outliers compared to RMSE.

The selection of the appropriate performance metric depends on the regression model and the characteristics of the dataset. By choosing the right metric, regression models can be effectively evaluated and optimised for real-world applications.

3.6 Final model evaluation

Four different regression models were trained in MATLAB, and the overall computational effort and training time were modest and very similar across all methods. After this training phase, the cross-validation and testing performance of each model was evaluated by calculating the performance metrics introduced in the previous subsection for the two cruise flight programmes.

As given in Tables 4 and 5, GPR consistently outperforms the other models across all evaluation criteria. For both cruise flight programmes, GPR achieves near-perfect coefficient of determination values $\left(R^2 \approx 1\right)$ in both the validation and testing phases, indicating that it explains almost all of the variance in the observed range data. Furthermore, GPR yields the lowest values in MSE, RMSE and MAE, signifying its superior predictive accuracy and reduced sensitivity to outliers.

These results highlight the effectiveness of GPR in capturing the underlying nonlinear relationships between flight parameters and cruise range. The probabilistic nature of GPR allows both accurate prediction and quantification of uncertainty, which is particularly advantageous in aeronautical applications where operational robustness is critical. Considering its consistent and superior performance across both cruise flight programmes, GPR is deemed the most suitable regression model for the aircraft range modeling task undertaken in this study.

Then, further diagnostic analysis is conducted using *predicted vs. actual plots* and *residuals plots* for both the validation and testing phases. These plots serve as essential tools for visually evaluating model performance beyond numerical metrics. The predicted vs. actual plot allows an assessment of overall prediction accuracy; ideally, data points should align closely with the 45-degree line, indicating strong agreement between predicted and true range values. Deviations from this line reveal systematic errors or model bias. The residuals plot, which displays the difference between actual and predicted values (i.e. residuals) against the true values, is used to examine the distribution of prediction errors. A well-behaved model typically exhibits residuals that are randomly scattered around zero without discernible patterns, suggesting that the model captures the underlying structure of the data without systematic bias.

https://doi.org/10.1017/aer.2026.10157 Published online by Cambridge University Press

Table 5. *Cross-validation and test performance results for the constant altitude and constant lift coefficient cruise*

		Regression model			
		DTR	SVR	GPR	NNR
Validation	R^2	0.93	0.99	≈ 1	≈ 1
	MSE	132,314	12,988	5.15	24.33
	RMSE	363.75	113.96	2.27	4.93
	MAE	306.34	101.48	1.6	3.89
Test	R^2	0.95	0.99	≈ 1	≈ 1
	MSE	88,483	13,162	5.64	25.21
	RMSE	297.46	114.73	2.37	5.02
	MAE	245.59	103.87	1.62	4.00

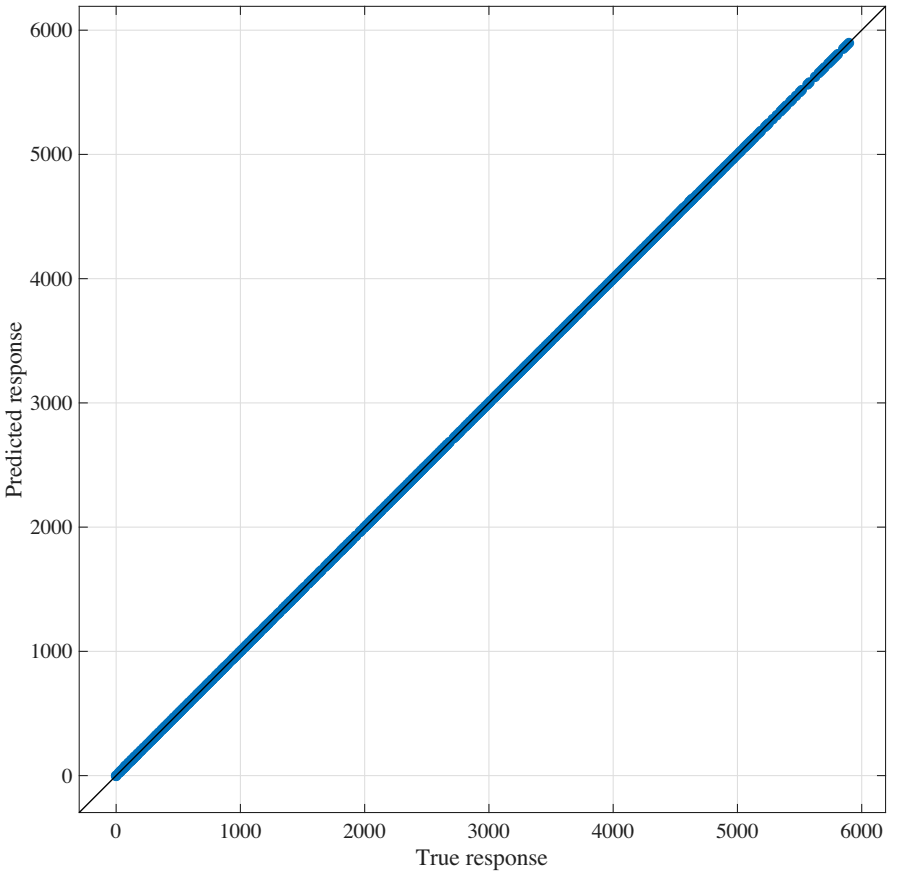


Figure 2. *Cross-validation results of predicted vs actual values with GPR model for the constant velocity and constant lift coefficient cruise.*

As shown in Figs 2–9, GPR exhibits strong agreement between predicted and actual values during both validation and testing phases, with minimal and homogeneously distributed residuals. This confirms that the model generalises well and does not suffer from overfitting or underfitting. These visual assessments reinforce the conclusion that GPR provides highly satisfactory performance for regression-based modeling of the aircraft cruise range under varying flight conditions.

https://doi.org/10.1017/aer.2026.10157 Published online by Cambridge University Press

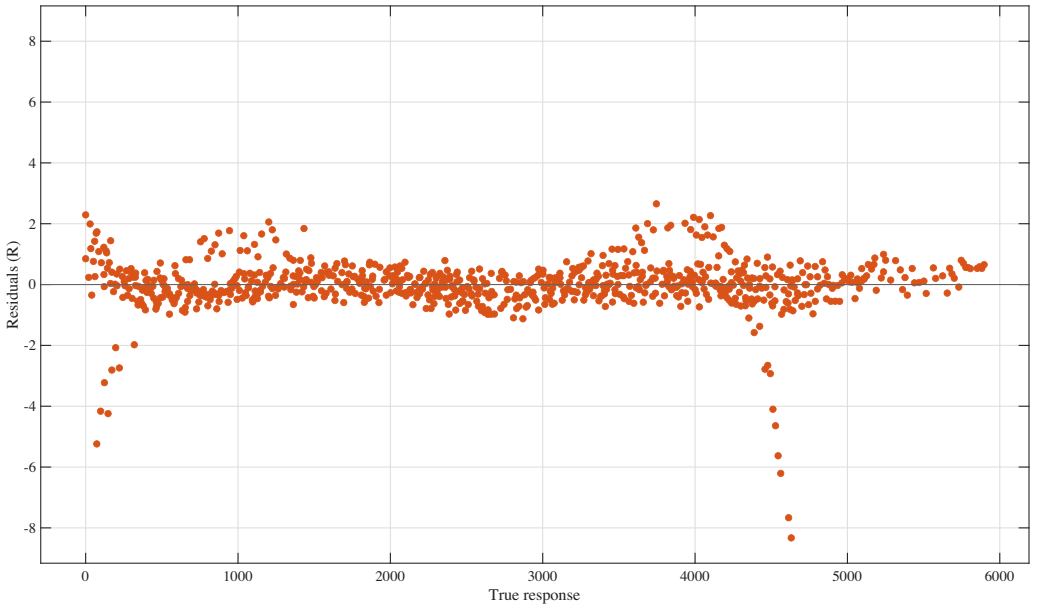


Figure 3. *Cross-validation results of residuals values with GPR model for the constant velocity and constant lift coefficient cruise.*

3.7 Model interpretation

While the regression models demonstrate satisfactory statistical accuracy, it is essential to assess whether the learned input–output relationships also reflect known physical dependencies. To this end, Shapley Additive Explanations (SHAP) analysis was applied to the final GPR models to quantify the relative importance of the predictor variables. The mean absolute SHAP values presented in Figs 10 and 11 indicate that altitude and aircraft weight are the dominant factors in the cruise range, while true airspeed has a significantly lower but still notable influence.

These results are fully consistent with aerodynamic expectations. Higher aircraft weight leads to increased fuel consumption and therefore reduced cruise range, a trend clearly captured by the model. Conversely, altitude exerts a strong positive influence up to intermediate values, reflecting the well-known fact that reduced air density at higher altitudes improves aerodynamic efficiency, but with diminishing benefit at very high altitudes where engine performance may degrade. The role of true airspeed is also physically interpretable: range predictions exhibit higher sensitivity in the constant altitude and constant lift coefficient cruise (see Fig. 11), as changes in Mach number directly affect both thrust-specific fuel consumption and drag characteristics.

Overall, the SHAP analysis demonstrates that the machine learning framework does not function as a purely statistical black box. Instead, it embeds meaningful aerodynamic relationships that align with established performance theory. This interpretability confirms that the regression models provide physical insight into the cruise range behaviour of the Boeing 737–400.

4.0 Comparison of machine learning model with analytical range formulas

In this section, a baseline comparison is carried out between the machine learning predictions and the classical analytical range formulas introduced in Section 2. The purpose of this comparison is not to validate the machine learning model in a strict quantitative sense, since the Bréguet-type equations rely on several simplifying assumptions, but rather to provide physical context and to examine whether the overall trends predicted by the regression model are consistent with well-known analytical behaviour. To this end, the analytical range expressions in Equations (1) and (3) are evaluated using the corresponding

https://doi.org/10.1017/aer.2026.10157 Published online by Cambridge University Press

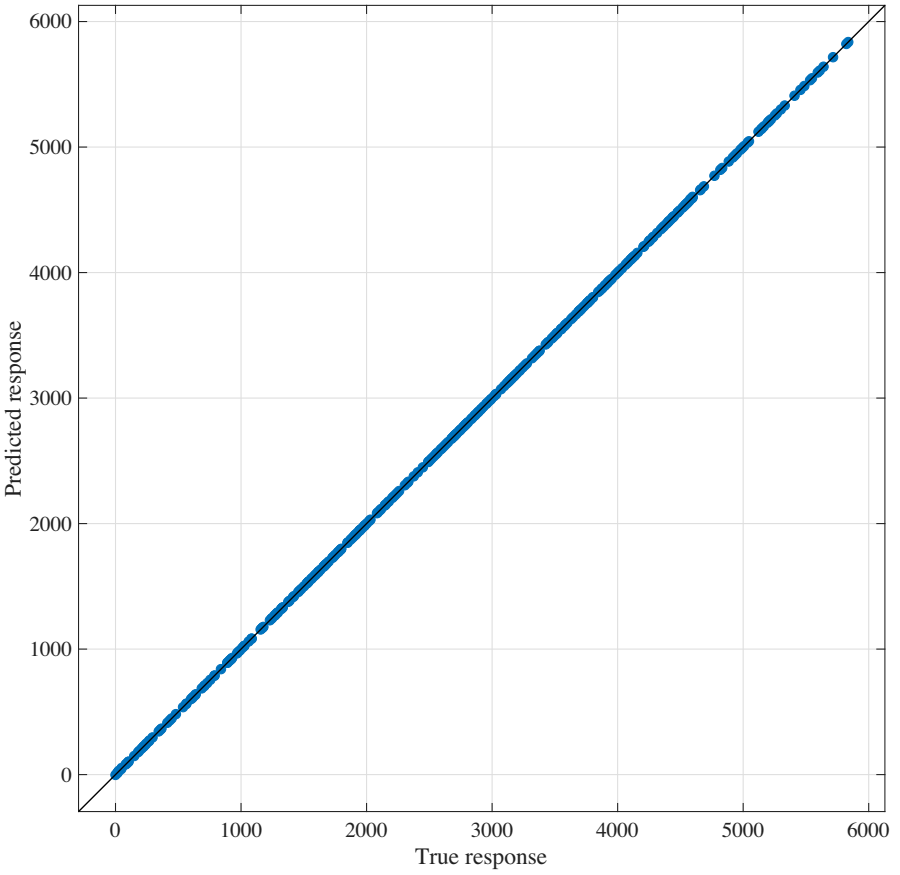


Figure 4. *Testing results of predicted vs actual values with GPR model for the constant velocity and constant lift coefficient cruise.*

values of weight, altitude and airspeed taken from the Operations Manual, and the resulting analytical ranges are compared with the machine learning-based predictions.

So as to accomplish the calculations of analytical range formulations, the following procedure is adopted:

i) Obtain the values of altitude, velocity, and initial/final weights of the aircraft from the Operations Manual.

ii) Compute ρ at the given altitude.

iii) Compute C_L from the lift equation.

iv) Compute C_D from the drag polar, then L/D.

v) Compute range with (1) and (3) using an appropriate approximation of c_T.

(ii) Combining the ISA model pressure and temperature formulas, the air density is given as:

(ii-a) For troposphere (0–11 km),

$$\rho\,(h) = \rho_0\left(1 - \frac{Lh}{T_0}\right)^{\left(\frac{g}{RL}-1\right)} \tag{13}$$

where ρ_0 and T_0 denote sea-level air density and temperature, respectively, as given by the ISA model. Furthermore, L, g, and R are the lapse rate, gravitational acceleration and universal gas constant, respectively. Since

$$\frac{g}{RL} - 1 = 4.25588,$$

https://doi.org/10.1017/aer.2026.10157 Published online by Cambridge University Press

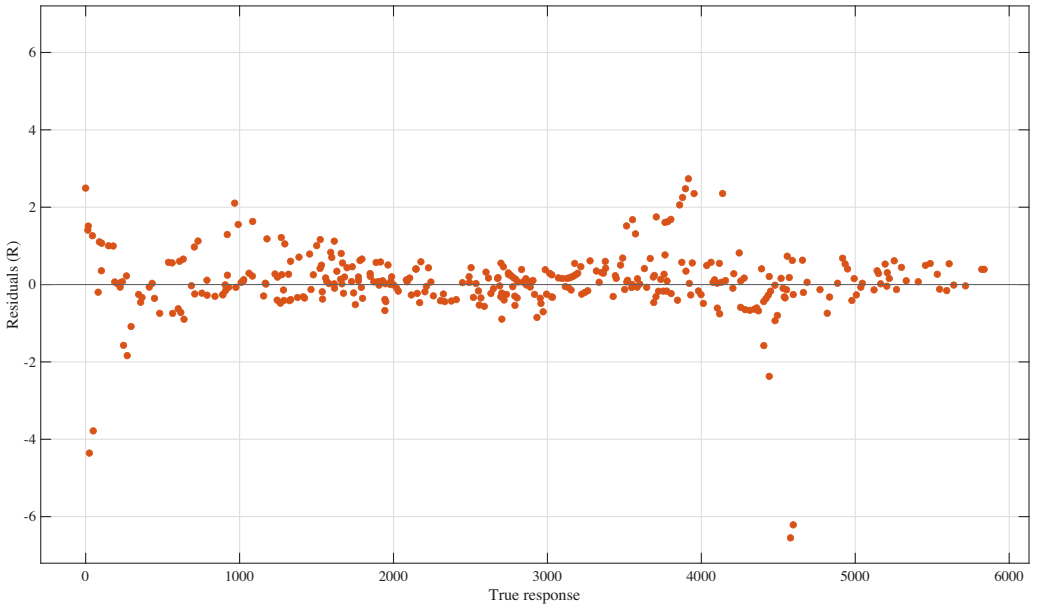


Figure 5. *Testing results of residuals values with GPR model for the constant velocity and constant lift coefficient cruise.*

then

$$\rho\,(h) = \rho_0\left(1 - 0.0065\frac{h}{288.15}\right)^{4.25588} \tag{14}$$

with $\rho_0 = 1.225 kg/m^3$.

ii-b) For stratosphere (11–20 km),

$$\rho\,(h) = \rho_{11} e^{\left(-\frac{g}{RT_{11}}(h-11000)\right)} \tag{15}$$

with $\rho_{11} = 0.36391 kg/m^3$.

(iii) For steady cruise flight, since lift balances weight ($L = W$), the lift coefficient is computed as

$$C_L = \frac{2W}{\rho V^2 S}, \tag{16}$$

where ρ is the ambient air density obtained from the ISA model at the corresponding altitude.

(iv) Despite the limitations discussed in Subsection 2.1, a quadratic drag polar of the form (5) is adopted for the analytical range calculations. In Ref. [35], drag polars for several commercial airliners are estimated from ADS-B data and compared with those provided in BADA 3 [36]. For the Boeing 737–400 (B734), the clean-configuration coefficients are reported approximately as $C_{D0} = 0.021$ and $K = 0.0372$.

The induced drag coefficient is commonly expressed as

$$K = \frac{1}{\pi AR\, e}, \tag{17}$$

where AR denotes the wing aspect ratio and e is the Oswald efficiency factor. For the Boeing 737–400 [37], reports $AR = 9.17$ and $e = 0.93$, which yield a K value of the same order of magnitude as the estimate provided in Ref. [35].

https://doi.org/10.1017/aer.2026.10157 Published online by Cambridge University Press

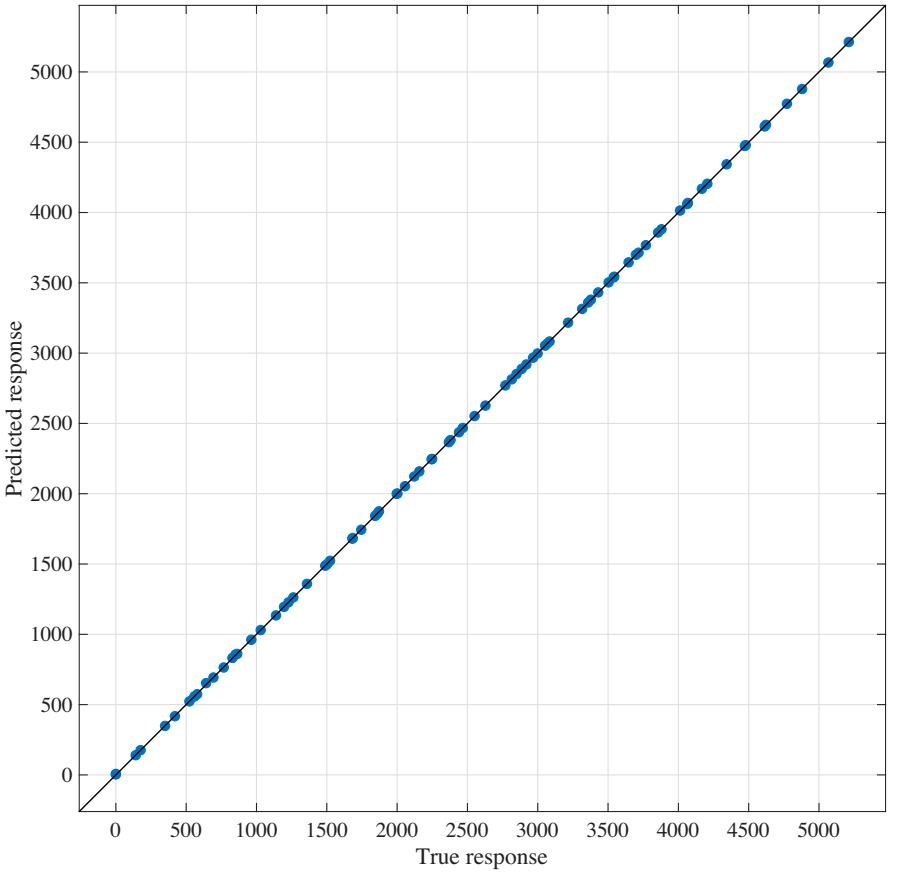


Figure 6. *Cross-validation results of predicted vs actual values with GPR model for the constant altitude and constant lift coefficient cruise.*

In the calculation of L/D, the calculated values of C_L and C_D are used for both cruise flight programmes. So,

$$\frac{L}{D} = \frac{C_L}{C_D}. \tag{18}$$

(v) In Ref. [38], a detailed energy-exergy analysis for the CFM56-3 series turbofan engines is performed using real engine data. In our study, for the analytical baseline, c_T during cruise is computed using a conventional thrust-based formulation and a representative calibrated value is chosen:

$$c_T = \frac{\dot{m}_f}{T}$$

where $\dot{m}_f$ indicates fuel mass flow and T is the engine thrust.

The range values computed from the analytical formulations in (1) and (3) are shown in Figures 12 and 13 for the constant velocity and constant lift coefficient cruise, and for the constant altitude and constant lift coefficient cruise, respectively. It should be emphasised that the results of the analytical range formulations serve as a trend baseline, not a high-fidelity performance model. It should be noted that Fig. 12 presents range behaviour at reference climb–cruise altitudes, rather than at a fixed level-flight altitude.

As shown in Fig. 12, the Bréguet range results obtained from (1) agree reasonably well with the Operations Manual values at lower aircraft weights. However, as weight increases, the analytical

https://doi.org/10.1017/aer.2026.10157 Published online by Cambridge University Press

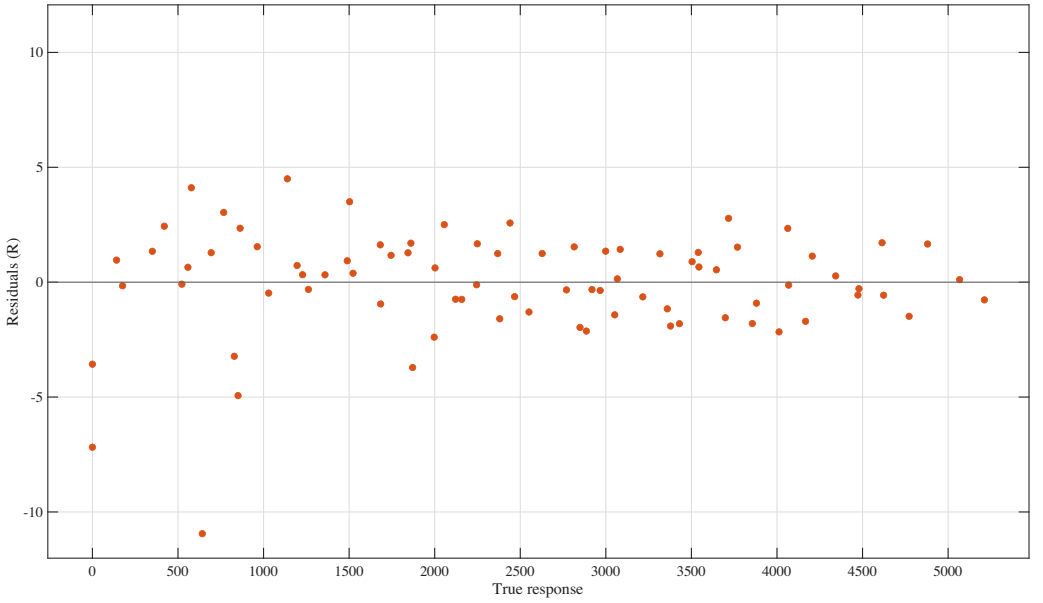


Figure 7. *Cross-validation results of residuals values with GPR model for the constant altitude and constant lift coefficient cruise.*

calculations begin to deviate noticeably from the real range data. This trend is expected because higher aircraft weights correspond to lower cruise altitudes where air density is greater. At these altitudes, turbofan thrust exhibits a stronger dependence on true airspeed, hence the simplified and calibrated c_T model, combined with the quadratic drag polar approximation, cannot fully capture this sensitivity. Consequently, the analytical formulation underestimates the influence of thrust variation and produces increasing discrepancies at higher weights. In contrast, the predicted range values align almost perfectly with the Operations Manual data across the entire weight range, indicating that the data-driven model successfully captures the underlying nonlinear relationships, which are neglected by the analytical formulation.

Beyond the overall agreement, Fig. 12 also reveals a clear altitude-dependent variation in the slope of the range–weight curves. At lower reference altitudes, the range decreases more rapidly with increasing weight, reflecting the higher air density and increased drag sensitivity, a behaviour consistent with classical cruise performance theory and the findings of Ref. [12]. This trend is captured by both the Operations Manual data and the machine learning–based predictions.

At higher reference altitudes, the range–weight curves exhibit a reduced slope, indicating improved aerodynamic efficiency due to lower air density, again in agreement with Ref. [12]. While the analytical formulation reproduces the general tendency, its reliance on simplified thrust-specific fuel consumption and quadratic drag polar assumptions leads to increasing discrepancies at higher weights. In contrast, the machine learning model preserves the altitude-dependent slope behaviour observed in the manufacturer data, further reinforcing its physical consistency.

A similar behaviour is observed in Fig. 13 for the constant altitude and constant lift coefficient cruise. For a fixed altitude, the deviation between analytical and real range values increases as flight speed rises. This occurs because the thrust required becomes more sensitive to true airspeed at higher velocities, amplifying the limitations of the simplified propulsion and aerodynamic models. The discrepancy is even more pronounced at lower altitudes, where air density is higher and the thrust variation with airspeed is more significant. Again, the machine-learning predictions closely match the Operations Manual values, demonstrating their ability to represent the combined aerodynamic and propulsion effects that are not fully captured by the analytical expressions.

https://doi.org/10.1017/aer.2026.10157 Published online by Cambridge University Press

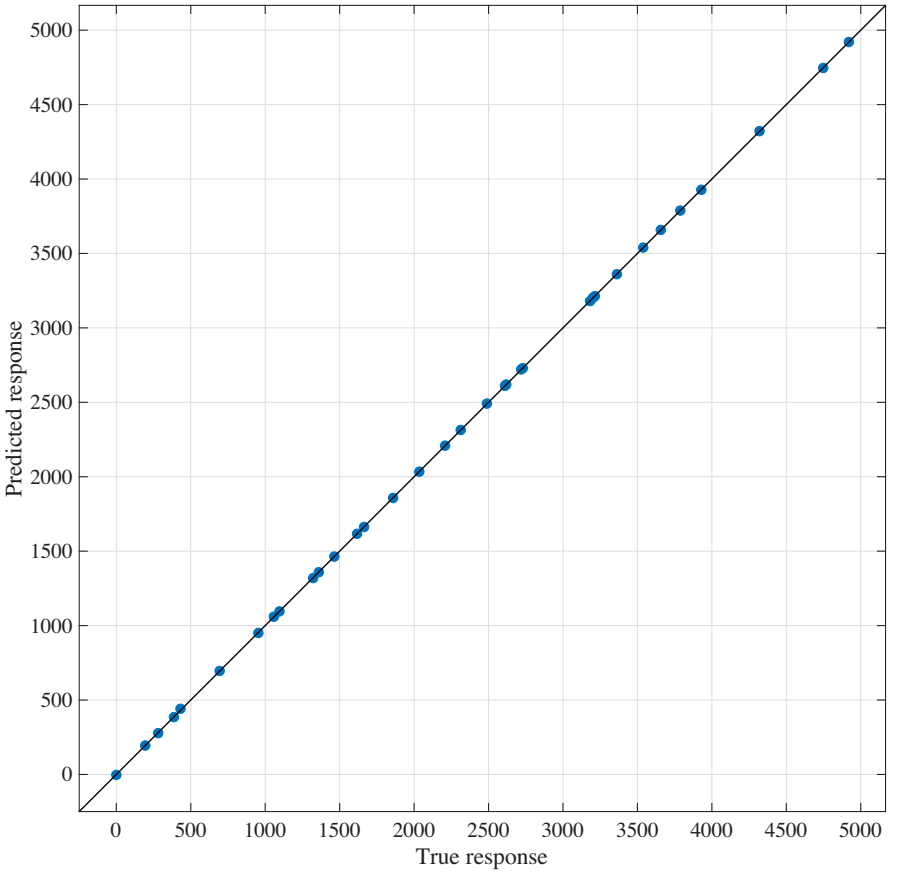


Figure 8. *Testing results of predicted vs actual values with GPR model for the constant altitude and constant lift coefficient cruise.*

Figure 13 further illustrates the altitude-dependent behaviour of the range and speed relationship. For a given altitude, the slope of the range curve changes nonlinearly with increasing true airspeed, indicating the competing effects of induced and parasite drag. At lower speeds, range is reduced due to higher induced drag, while at higher speeds, increasing parasite drag and fuel flow lead to a steeper reduction in range. This characteristic behaviour is consistent with classical cruise performance analyses and the trends reported in Ref. [13].

The altitude dependence of this behaviour is also evident, as lower altitudes exhibit stronger slope variations due to higher air density and increased thrust sensitivity to airspeed. While the analytical formulation captures the general trend, its simplified aerodynamic and propulsion assumptions limit its ability to accurately represent these slope changes across the full speed range. In contrast, the machine learning model closely follows the altitude-dependent range–speed tendencies observed in the Operations Manual data, reinforcing its physical consistency and validity.

5.0 Prediction for unseen data

The prediction workflow, shown in Fig. 14, begins by normalising the unseen predictor inputs using the same z-score parameters (mean and variance) recorded during the initial modeling phase. This step ensures consistency and allows the new input values to be processed in a manner that aligns with the

https://doi.org/10.1017/aer.2026.10157 Published online by Cambridge University Press

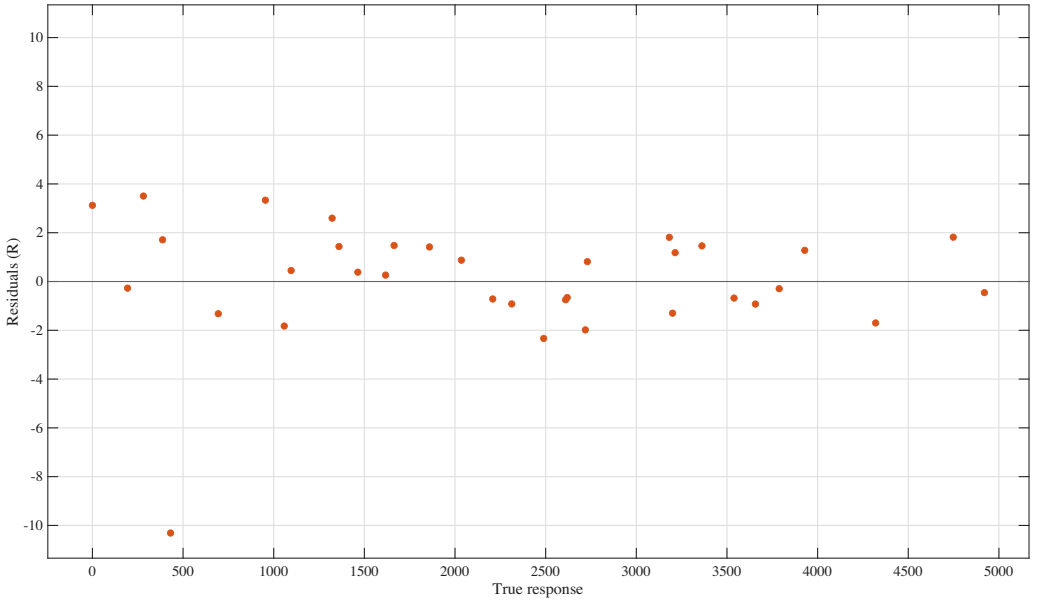


Figure 9. *Testing results of residuals values with GPR model for the constant altitude and constant lift coefficient cruise.*

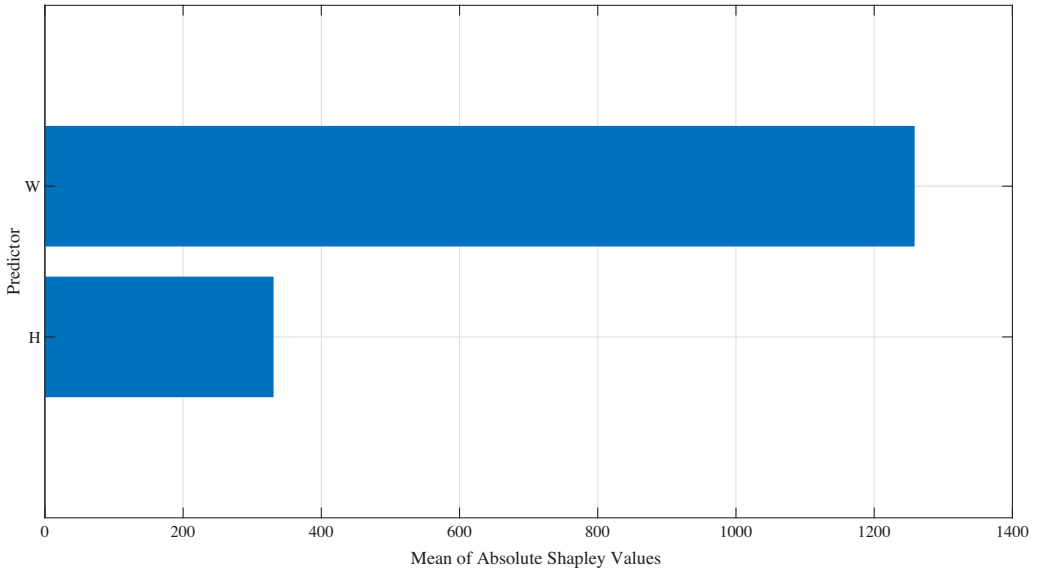


Figure 10. *Shapley importance values of GPR model for the constant velocity and constant lift coefficient cruise.*

internal representation of the trained model. The normalised input vectors are then fed into the final GPR model to obtain the predicted cruise range values.

To demonstrate the generalisation capability of the developed regression models and to explore the aircraft's range behaviour under a broader set of conditions, a set of unseen input data has been introduced, consisting of varying weight and speed combinations at three additional cruise altitudes for each cruise flight programmes. Since the GPR model has demonstrated excellent predictive accuracy and

https://doi.org/10.1017/aer.2026.10157 Published online by Cambridge University Press

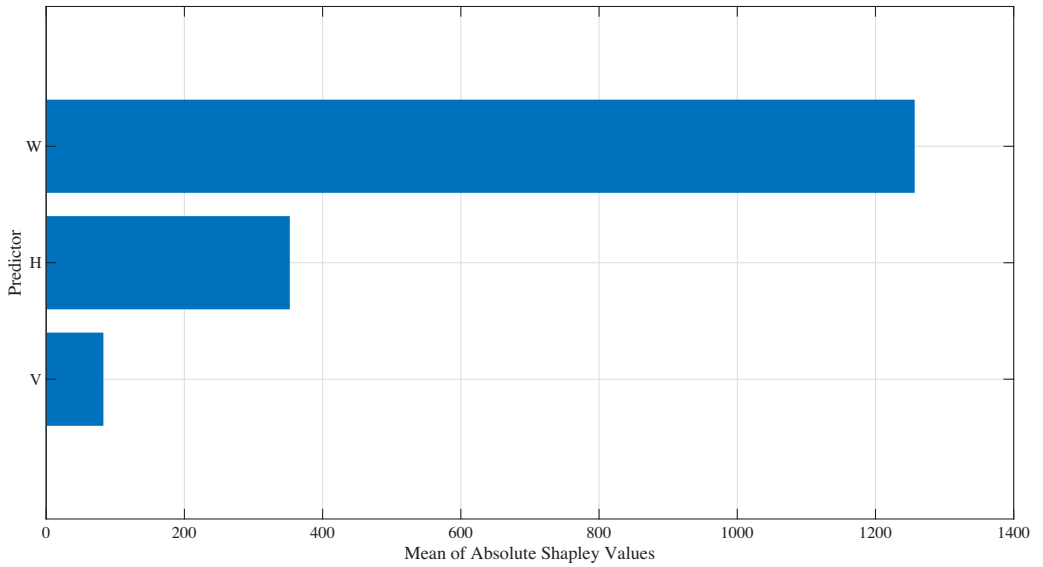


Figure 11. *Shapley importance values of GPR model for the constant altitude and constant lift coefficient cruise.*

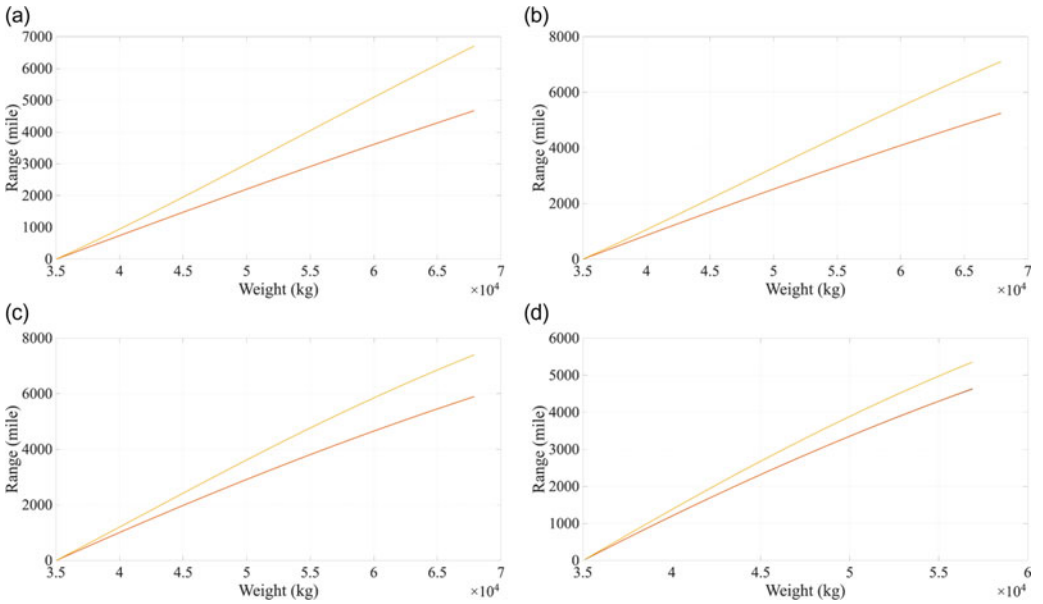


Figure 12. *Real (blue line), predicted (red line) and calculated (yellow line) range values for altitude (a) 21,000 ft, (b) 25,000 ft, (c) 30,000 ft and (d) 37,000 ft. The real and predicted curves are almost perfectly aligned, making it difficult to distinguish the two lines despite their different colours.*

generalisation performance, it is well-suited for this exploratory analysis. The purpose of this exercise is to examine the possible range dynamics of the aircraft under different operational scenarios that extend beyond the initially available data.

First, the constant velocity and constant lift coefficient cruise is considered. This flight programme corresponds to a climb–cruise in which the aircraft continuously increases its altitude as fuel is burned,

https://doi.org/10.1017/aer.2026.10157 Published online by Cambridge University Press

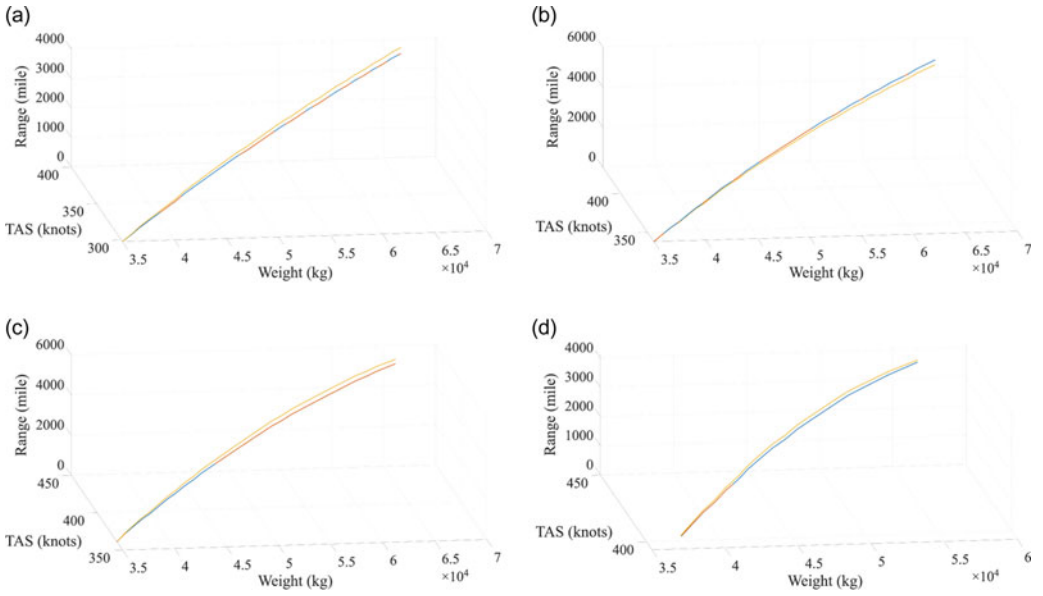


Figure 13. *Real (blue line), predicted (red line) and calculated (yellow line) range values for altitude (a) 10,000 ft, (b) 20,000 ft, (c) 25,000 ft and (d) 30,000 ft. The real and predicted curves are almost perfectly aligned, making it difficult to distinguish the two lines despite their different colours.*

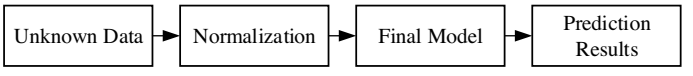


Figure 14. *Prediction workflow.*

rather than operating at a fixed altitude. However, the Operations Manual reports cruise performance data at discrete reference altitude levels that characterise representative climb–cruise conditions. Based on these reference levels, unseen input data were generated at intermediate altitudes of 23,000 ft, 28,000 ft and 35,000 ft, which lie between the tabulated altitudes in the training set. These altitudes should be interpreted as interpolation points between nominal climb–cruise reference conditions rather than as fixed cruising altitudes. The resulting predictions are shown in Fig. 15, illustrating how range varies with aircraft weight across these intermediate reference altitude levels.

The surface shown in Fig. 15 illustrates how range varies with aircraft weight at different cruise altitudes. The results should be interpreted as range behaviour associated with reference climb–cruise altitude levels, rather than steady level flight at a fixed altitude. As expected, increasing weight (while assuming the same amount of fuel) reduces the achievable range due to higher fuel consumption, while higher altitudes yield improved range efficiency up to a certain level. This trend reflects the aerodynamic advantage of reduced drag at mid-to-high altitudes, consistent with classical performance theory.

Then, the constant altitude and constant lift coefficient cruise is evaluated. A set of unseen cruise flight data is created for altitudes of 15,000 ft, 22,500 ft and 27,000 ft with varying weight and velocity values. The resulting predictions, visualised in Figs 16 and 17, are plotted from different angles. Figures 16 and 17 provide 2D slices of the prediction surface in the constant altitude and constant lift coefficient cruise. The plots clearly demonstrate that range decreases monotonically with increasing weight, while the effect of true airspeed is nonlinear. At lower speeds, range is reduced due to higher induced drag, whereas excessively high speeds also degrade range because of increased parasite drag and fuel flow. The model therefore captures the existence of an optimal speed interval. Taken together, these surfaces confirm that the machine learning model embeds realistic aerodynamic trade-offs between weight, altitude and speed, thereby supporting its physical interpretability.

https://doi.org/10.1017/aer.2026.10157 Published online by Cambridge University Press

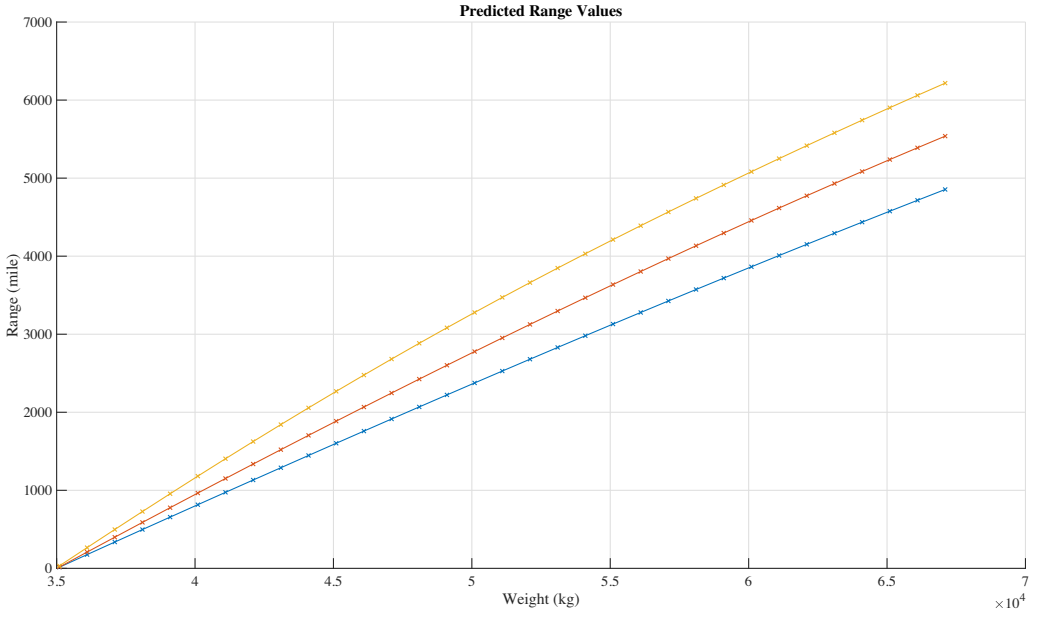


Figure 15. *Predicted range values for altitude 23,000 ft (blue crosses), 28,000 ft (red crosses) and 35,000 ft (yellow crosses).*

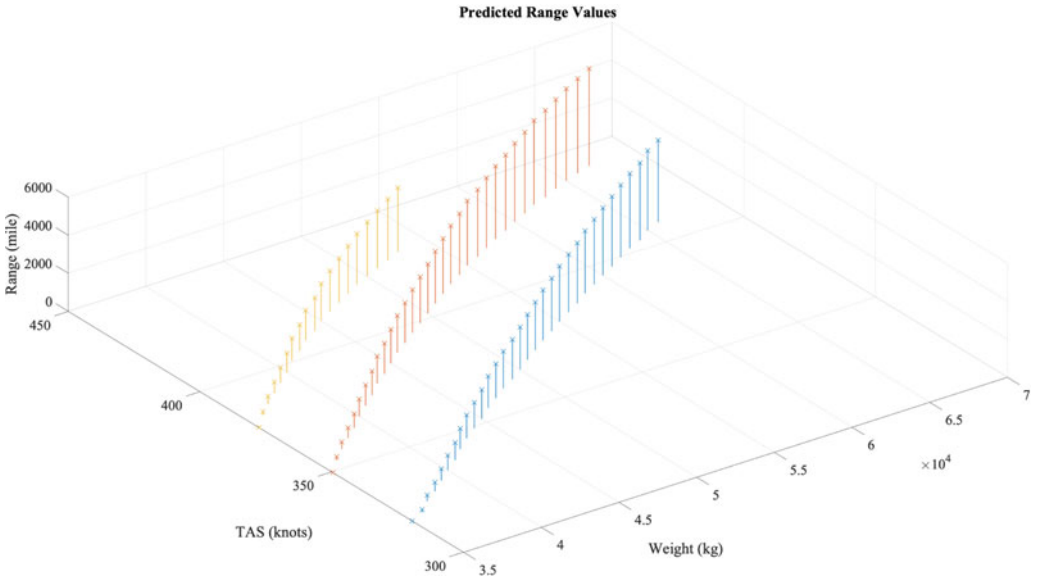


Figure 16. *Predicted range values for altitude 15,000 ft (blue crosses), 22,500 ft (red crosses) and 27,000 ft (yellow crosses).*

These predictions provide valuable insight into the range performance of the aircraft in new cruise flight programmes, underscoring the practical applicability of the developed regression model. Furthermore, they also enable a data-driven exploration of how cruise range varies with aircraft weight, speed and altitude, which are the factors that are critical to fuel efficiency, emissions and operational planning as previously emphasised in the introduction.

https://doi.org/10.1017/aer.2026.10157 Published online by Cambridge University Press

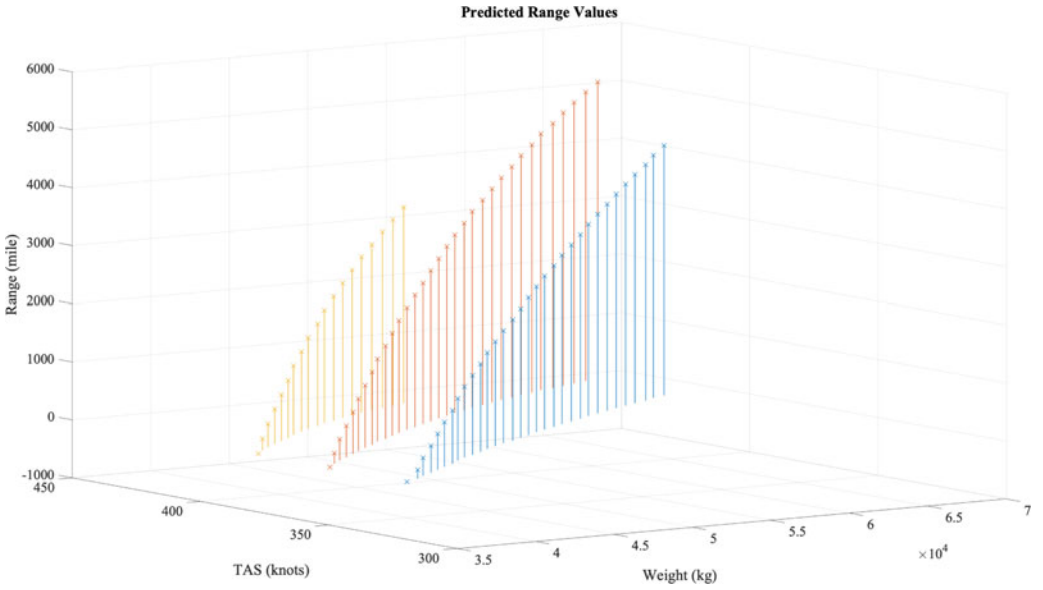


Figure 17. *Predicted range values for altitude 15,000 ft (blue crosses), 22,500 ft (red crosses) and 27,000 ft (yellow crosses).*

It should be noted that GPR is primarily an interpolation method and may yield unreliable extrapolations outside the training domain. In the present study, however, the prediction results do not represent extrapolation. The GPR model developed for the constant velocity and constant lift coefficient cruise was trained with altitude values of 21,000 ft, 25,000 ft, 30,000 ft and 37,000 ft, while the predictions, illustrated in Fig. 11, were evaluated at 23,000 ft, 28,000 ft and 35,000 ft. Similarly, the prediction datasets used for the constant altitude and constant lift coefficient cruise were designed in the same manner: while the training data included altitudes of 10,000 ft, 20,000 ft, 25,000 ft and 30,000 ft, the prediction phase was performed for 15,000 ft, 22,500 ft and 27,000 ft, as illustrated in Figs 12 and 13. These lie within the convex hull of the training set, and thus the model is performing interpolation rather than extrapolation. The prediction datasets were also carefully created to be consistent with the flight envelope of the Boeing 737–400, ensuring that all interpolated conditions are operationally meaningful. In addition, the weight ranges used in the latter dataset were explicitly constrained not to exceed the maximum takeoff weight of the Boeing 737–400, thereby ensuring physical realism. As expected, the predicted trends are smooth and physically consistent across these intermediate operating conditions. Nevertheless, we emphasise that caution should be exercised when applying GPR beyond the trained input space, as the associated uncertainty may increase and the predictions may not remain physically reliable.

6.0 Conclusion

This study has demonstrated the efficiency of machine learning-based regression techniques for modeling the cruise range of a jet-powered transport aircraft under two distinct cruise flight programmes. To the authors' best knowledge, this research introduces the first aircraft range models utilising machine learning in current literature. In contrast to conventional analytical and optimisation-based methods, the proposed data-driven approach offers improved accuracy, robustness and flexibility. Among the tested models, GPR consistently outperformed alternatives in both cross-validation and test phases, yielding near-perfect predictive performance.

https://doi.org/10.1017/aer.2026.10157 Published online by Cambridge University Press

In addition, the developed models were also subjected to interpretability analysis using SHAP values. This analysis confirmed that the models reproduce physically meaningful dependencies such as reduced range at higher weights and enhanced efficiency at intermediate altitudes. This outcome is consistent with established aerodynamic principles. Therefore, the proposed machine learning approach provides not only statistical accuracy but also valuable physical insight into aircraft cruise range behaviour.

Using the GPR model, the range dynamics of the aircraft is successfully explored in new flight conditions not present in the original dataset. The results confirm that machine learning regression can serve as a powerful tool in modern aeronautical performance analysis and strategic flight planning. In addition, the comparisons conducted in Section 4 demonstrate that the machine learning predictions capture the physical tendencies expected from classical range theory while also accounting for effects not represented in the analytical formulations.

In addition to the predictions presented in this study, the developed models can be used:

- To obtain *operational climb-cruise profile* by simulating a realistic step climb profile where altitude increases gradually during cruise while maintaining constant velocity and lift coefficient. The predicted range evolution along this path can approximate real-world climbing cruise operations in the case of suitable air-traffic management conditions.
- To obtain *fuel efficiency mapping across operational envelope*, which generates a range-per-fuel-consumed map (i.e. specific range) by combining predicted range with estimated fuel weight differences incorporating an accurate fuel flow rate model. This can guide optimal cruise levels for fuel efficiency.
- To obtain *operational envelope limits identification* by identifying critical points where predicted range starts to degrade sharply, e.g. at very high weights or low altitudes. These boundaries can define the aircraft's practical cruise range envelope under constant velocity and constant lift coefficient cruise. However, it should be noted that an accurate aircraft thrust model would be needed to combine with the developed range model.

Acknowledgment. The authors acknowledge the use of AI tools (specifically ChatGPT, powered by OpenAI's language model GPT-5.1; http://openai.com) for language-related improvements, including proofreading, grammar refinement and enhancing the clarity of written English. After using AI tools, the authors reviewed and edited the content as needed and take full responsibility for the content of the published article.

References

[1] Saarlas, M. Aircraft Performance, John Wiley & Sons, 2007, Hoboken, NJ, USA.
[2] Oruc, R. and Baklacioglu, T. Modeling of fuel flow-rate of commercial aircraft for the descent flight using particle swarm optimization, *Aircr. Eng. Aerosp. Technol.*, 2021, **93**, (2), pp 319–326. doi:10.1108/AEAT-09-2020-0213
[3] Turgut, E.T., Cavcar, M., Usanmaz, O., Canarslanlar, A.O., Dogeroglu, T., Armutlu, K. and Yay, O.D., Fuel flow analysis for the cruise phase of commercial aircraft on domestic routes, *Aerosp. Sci. Technol.*, 2014, **37**, pp 1–9. doi:10.1016/j.ast.2014.04.012
[4] Baklacioglu, T. Modeling the fuel flow-rate of transport aircraft during flight phases using genetic algorithm-optimized neural networks, *Aerosp. Sci. Tech.,* 2016, **49,** pp 52–62. doi:10.1016/j.ast.2015.11.031
[5] Marinus, B.G. and Hauglustaine, A. Data-driven modeling of fuel consumption for turboprop-powered civil airliners, *Energies,* **13**, 2020, (7), p 1695. doi:10.3390/en13071695
[6] Fang, S., Qu, C. and Liu, T. Prediction of aircraft fuel consumption based on machine learning algorithm, in: 2024 International Conference on Aerospace and Mechanics, Vol. 2882, IOP Publishing, 2024, p. 012043. doi:10.1088/1742-6596/2882/1/012043
[7] Edwards, H., Dixon-Hardy, D. and Wadud, Z. Optimisation of aircraft cost indices to reduce fuel use, in: Proceedings of the 94th Annual Meeting of the Transportation Research Board, Transportation Research Board, Washington, DC, USA, 2015, paper presented at TRB 94th Annual Meeting. URL http://eprints.whiterose.ac.uk/91133/
[8] Zaporozhets, O. and Synylo, K. Improvements on aircraft engine emission and emission inventory assessment inside the airport area, *Energy,* 2017, **140**, pp 1350–1357. doi:10.1016/j.energy.2017.07.178
[9] Cecen, R.K. Flight regimes and environmental impact: a linear regression analysis of co2 emissions for en-route air traffic operations, *Int. J. Aeronaut. Space Sci.* **26**, 2058–2069. doi:10.1007/s42405-024-00860-z

https://doi.org/10.1017/aer.2026.10157 Published online by Cambridge University Press

[10] Graver, B., Rutherford, D. and Zheng, S. Co2 emissions from commercial aviation: 2013, 2018, and 2019, Tech. rep., International Council on Clean Transportation (ICCT), Washington, DC, USA (2020). URL https://theicct.org/publications/co2-emissions-commercial-aviation-oct2020
[11] Dinc, A. and Otkur, M. Emissions prediction of an aero-piston gasoline engine during surveillance flight of an unmanned aerial vehicle, *Aircr. Eng. Aerosp. Technol.*, 2021, **93**, (3), pp462–472. doi:10.1108/AEAT-09-2020-0196
[12] Cavcar, M. Breguet range equation?, *J. Aircr.*, 2006, **43**, (5), pp 1542–1544. doi:10.2514/1.17696
[13] Cavcar, A. Constant altitude–constant mach number cruise range of transport aircraft with compressibility effects, *J. Aircr.*, 2006, **43**, (1), pp 125–131. doi:10.2514/1.14252
[14] Cavcar, M. and Cavcar, A. Comparison of generalized approximate cruise range solutions for turbojet/fan aircraft, *J. Aircr.*, 2003, **40**, (5), pp 891–900. doi:10.2514/2.6879
[15] Cavcar, A. and Cavcar, M. Approximate solutions of range for constant altitude – constant high subsonic speed flight of transport aircraft, *Aerosp. Sci. Technol.,* 2004, **8** (6), pp 557–567. doi:10.1016/j.ast.2004.04.002
[16] Peckham, D.H. Range performance in cruising flight, Tech. Rep. Technical Report 73164, Royal Aircraft Establishment, Farnborough, England (1974).
[17] Torenbeek, E. Cruise performance and range prediction reconsidered, *Prog. Aerosp. Sci.*, 1997, **33**, pp 285–321. doi:10.1016/S0376-0421(96)00007-3
[18] Rivas, D., Lopez-Garcia, O., Esteban, S. and Gallo, E. An analysis of maximum range cruise including wind effects, *Aerosp. Sci. Technol.*, 2010, **14**, (1), pp 38–48. doi:10.1016/j.ast.2009.11.005
[19] Randle, W.E., Hall, C.A. and Vera-Morales, M. Improved range equation based on aircraft flight data, *J. Aircr.*, 2011, **48**, (4), pp 1291–1300. doi:10.2514/1.C031262
[20] Atasoy, V.E. and Cetek, C. Enhanced cruise range prediction for narrow-body turbofan commercial aircraft based on QAR data, *Aeronaut. J.*, 2021, **125**, (1286), pp 672–701. doi:10.1017/aer.2020.121
[21] Wislicenus, J. and Daidzic, N.E. Estimation of transport-category jet airplane maximum range and airspeed in the presence of transonic wave drag, *Aerospace*, 2022, **9**, (4), p 192. doi:10.3390/aerospace9040192
[22] Chati, Y.S. and Balakrishnan, H., Statistical modeling of aircraft takeoff weight, in: Twelfth USA/Europe Air Traffic Management Research and Development Seminar (ATM 2017), Seattle, WA, USA, 2017
[23] Sun, J., Ellerbroek, J. and Hoekstra, J.M., Aircraft initial mass estimation using bayesian inference method, *Transp. Res. C Emerg. Technol.*, 2018, **90**, pp 59–73. doi:10.1016/j.trc.2018.02.022
[24] Marinus, B.G. and Maison, J. Fuel weight estimates of military turbo-propeller transport aircraft, *Aerosp. Sci. Technol.*, 2016, **55**, pp 458–464. doi: 10.1016/j.ast.2016.06.019
[25] Parget, H. and Ardema, M.D. *Performance Analysis and Design of Flight Vehicles: Methods for Estimating Fuel Consumption and Range*, NASA Reference Publication, 2007, Washington, DC.
[26] Oruc, R. and Baklacioglu, T. Cruise range modeling of different flight strategies for transport aircraft using genetic algorithms and particle swarm optimization, *Energy*, 2024, **294**, p 130917. doi: 10.1016/j.energy.2024.130917
[27] Kim, D., Druot, T. and Liem, R.P. Data-driven operation-based aircraft design optimization, in: AIAA AVIATION 2020 FORUM, American Institute of Aeronautics and Astronautics, 2020. doi:10.2514/6.2020-3156
[28] Kim, D., Seth, A. and Liem, R.P. Data-enhanced dynamic flight simulations for flight performance analysis, *Aerosp. Sci. Technol.*, 2022, **121**, p 107357. doi:10.1016/j.ast.2022.107357
[29] Wang, M., Luiz, S.O.D., Zhang, S. and Lima, A.M.N. A range prediction method for all-electric aircraft by capacity discretization-based iterative convex programming, IEEE Trans. Transp. Electrification, 2024, **10**, (2), pp 3455–3469. doi:10.1109/TTE.2023.3298642
[30] Wroblewski, G.E. and Ansell, P.J. A Breguet range equation for hybrid-electric jet aircraft sizing and analysis, in: AIAA Propulsion and Energy 2020 Forum, American Institute of Aeronautics and Astronautics, 2020. doi:10.2514/6.2020-3579
[31] Group, B.C.A. Boeing 737–400 operations manual, Tech. rep. (1988).
[32] Betts, J.T. Survey of numerical methods for trajectory optimization, *J. Guid. Control Dyn.*, 1998, **21**, (2), pp 193–207.
[33] Rao, S.S. Engineering Optimization: Theory and Practice, 4th Edition, John Wiley & Sons, Hoboken, New Jersey, 2009.
[34] The MathWorks. Statistics and Machine Learning Toolbox, The MathWorks, Inc., Natick, Massachusetts, USA (2024). URL https://www.mathworks.com/products/statistics.html
[35] Sun, J., Hoekstra, J.M. and Ellerbroek, J. Aircraft drag polar estimation based on a stochastic hierarchical model, in: 8th SESAR Innovation Days, Salzburg, Austria, 2018, pp 1–8.
[36] EUROCONTROL. Base of aircraft data (bada) – version 3, User manual/aircraft performance model, European Organisation for the Safety of Air Navigation (EUROCONTROL) (2000). URL https://www.eurocontrol.int/model/bada
[37] Roskam, J. and Lan, C.E. Methods for Estimating Drag Polars of Subsonic Airplanes, Department of Aerospace Engineering, University of Kansas, Lawrence, Kansas, USA, 1997.
[38] Korba, P., Balli, O., Caliskan, H., Al-Rabeei, S. and Kale, U. Energy, exergy, economic, environmental, and sustainability assessments of the CFM56-3 series turbofan engine used in the aviation sector, *Energy,* 2023, **269**, p 126765. doi:10.1016/j.energy.2023.126765

Cite this article: Özer S.M. and Baklacioglu T. (2026). Cruise range modeling of a transport aircraft using machine learning. *The Aeronautical Journal*, **130**, 2293–2318. https://doi.org/10.1017/aer.2026.10157

https://doi.org/10.1017/aer.2026.10157 Published online by Cambridge University Press